eLIFE
elifesciences.org

Figures and figure supplements

Cortical regulation of cell size by a sizer cdr2p

Kally Z Pan, et al.

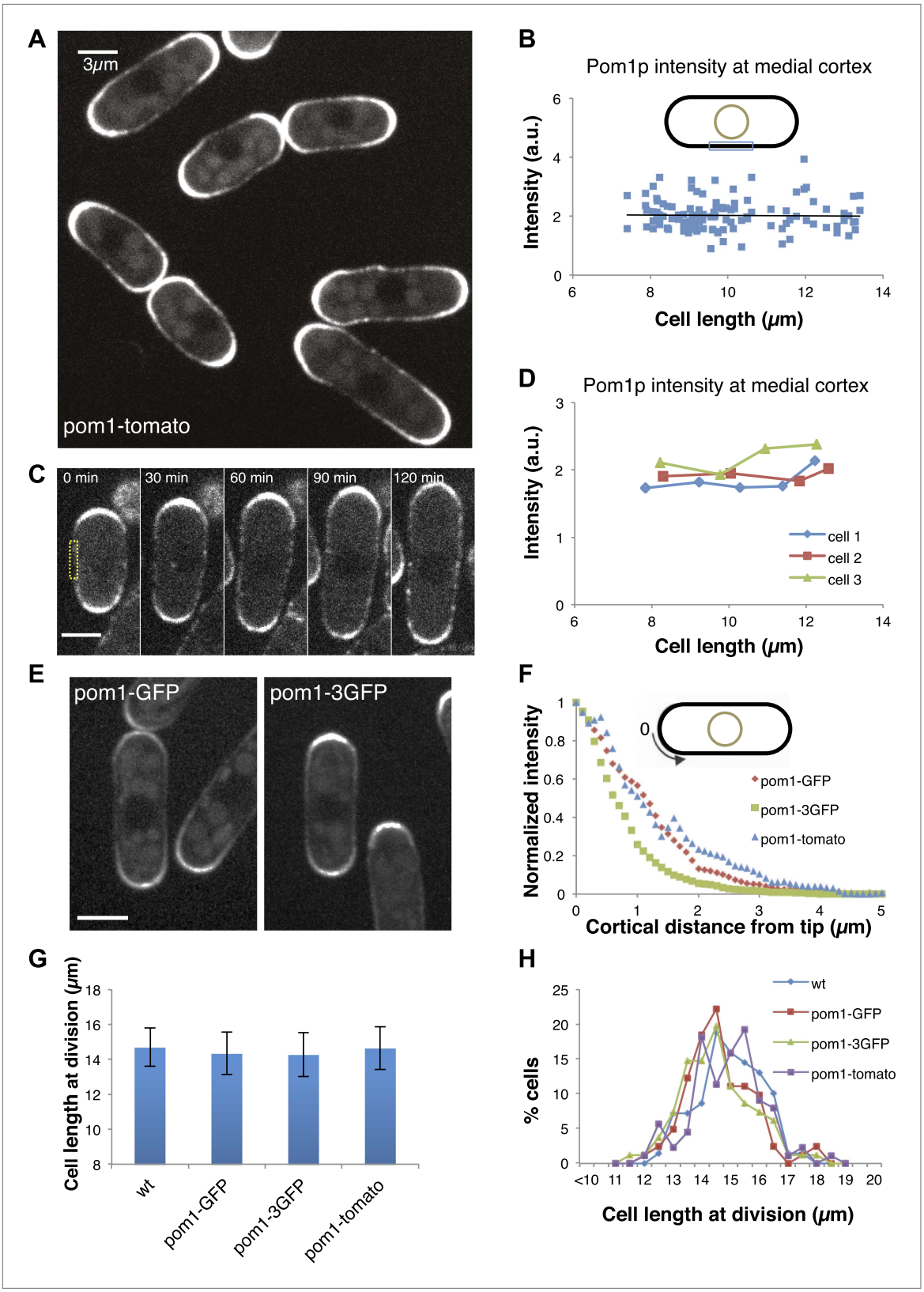

Figure 1. Gradient distribution of pom1p is not the basis for cell size control. (**A**) Time-averaged spinning disc confocal images of fission yeast cells expressing pom1-tomato in a medial focal plane (60 frames over 3 min). Scale bar = 3 μm. Strain used: FC2054. (**B**) Total fluorescence intensities of

Figure 1. Continued on next page

Figure 1. Continued

pom1-tomato in a medial 3-μm segment along cortical edge of interphase cells, from images like **A** (n > 100). See ***Figure 1—figure supplements 1–3***. (**C**) Time-lapse images of pom1-tomato in individual cell. Images are time averaged (5 frames over 25 s) in medial focal plane. Scale bar = 3 μm. (**D**) Pom1-tomato intensities at medial cortex (as in **B**) of individual growing interphase cells. (**E**) Cells expressing pom1-GFP or the pom1-3GFP. Imaging as in **A**. Strains used: FC1162, FC2685. Scale bar = 3 μm. (**F**) Gradient profiles of pom1-3GFP, pom1-GFP and pom1-tomato (n > 30 each strain). Peak absolute protein numbers in pom1-3GFP and pom1-GFP gradients were similar. Error bars not shown for clarity. See ***Figure 1—figure supplement 4***. (**G**) Effect of pom1p fusions on cell size as measured by length of septated cells (n > 100). Error bars: SDs. Strains used: FC420, FC1162, FC2685, FC2054. See ***Figure 1—figure supplement 4C, 5***. (**H**) Distribution of cell lengths at division in indicated strains.

DOI: 10.7554/eLife.02040.003

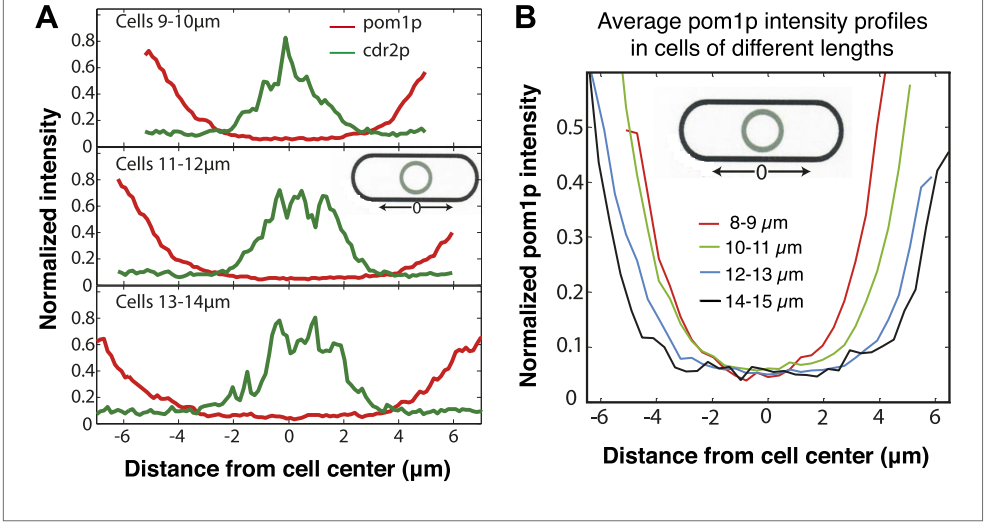

Figure 1—figure supplement 1. Pom1p concentration at the medial cortex does not vary with cell length. (**A**) Distributions of pom1p and cdr2p intensity around the cell cortex, measured as shown in the schematic. Cells co-expressing pom1-tomato and cdr2-GFP were imaged for 3 s in a confocal section through the middle of each cell, with a 20 s interval between time points (30 measurements in total) and the subsequent intensities time averaged. Average pom1p (red) and cdr2p (green) profiles for varying cell lengths are shown, normalized by the maximum value of pom1p and cdr2p time-averaged intensity recorded for an individual cell respectively. Top: n = 78 cells, middle n = 88 cells, bottom n = 32 cells. Note that cdr2p nodes reside in the low intensity region of the pom1p gradient at all cell lengths. Strain used: FC2678. (**B**) Profile of pom1p intensity gradients at different cell lengths, based on data shown in (**A**). The measurement region is shown in the schematic. Pom1p intensity profiles are normalized by the maximum average value in the entire set. n > 15 for each profile.

DOI: 10.7554/eLife.02040.004

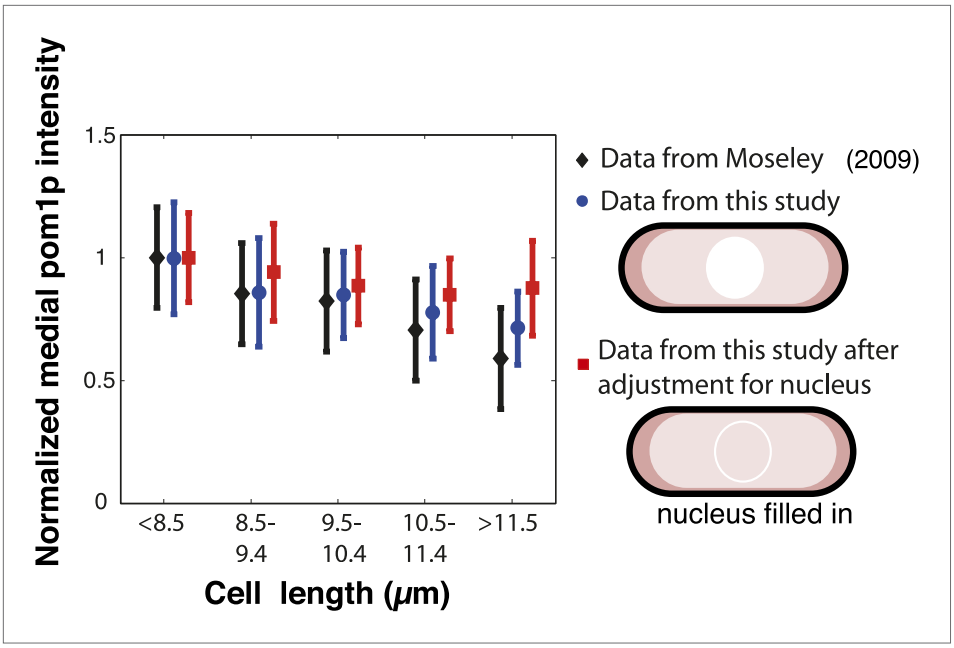

Figure 1—figure supplement 2. Pom1p concentration at the medial cortex: Comparison with previous data. ***Moseley et al. (2009)*** and ***Martin and Berthelot-Grosjean (2009)*** showed, in contrast to what we see, that pom1p levels in the middle of the cell decrease with cell length. In the measurements of these papers, pom1p fluorescence in the whole cell was collapsed onto a single line. This method of image analysis differs from our approach of measuring pom1p intensity only on the cortex, where the gradient distribution is shown in ***Figure 1*** and ***Figure 1—figure supplement 1***. We plotted measurements of pom1p in the middle of the cell as a function of cell length using different methods and data sets. The data from Moseley et al. (Figure S12 of that publication) is presented here (after normalization to the value for cells with length <8.5 μm) as the black bars. We found a similar trend using the same whole cell analysis on our own images of pom1-tomato cells (blue bars), n > 20 in each binning of cell lengths. pom1p is detectable at a low constant level all through the cytoplasm, but is not detectable in the nucleus (***Saunders et al., 2012***; ***Figure 1A***). Therefore, we tested whether this difference between whole cell and cortical measurements may be due to lack of pom1p in the nucleus. We adjusted for the effect of the nucleus by filling the nucleus with the average cytoplasmic pom1p intensity in silico. This adjustment largely abrogated the length-dependent decrease of pom1p intensity (red bars). We speculate that the decrease seen in the whole cell measurements may be due to the slightly larger size of the nucleus in larger cells (***Neumann and Nurse, 2007***; ***Figure 1—figure supplement 3***). Thus, the decrease seen in the previous publications may (partially) be an artifact of including cytoplasmic and nuclear fluorescence in addition to the cortical distribution. Strain used: FC2054. Error bars = SD.

DOI: 10.7554/eLife.02040.005

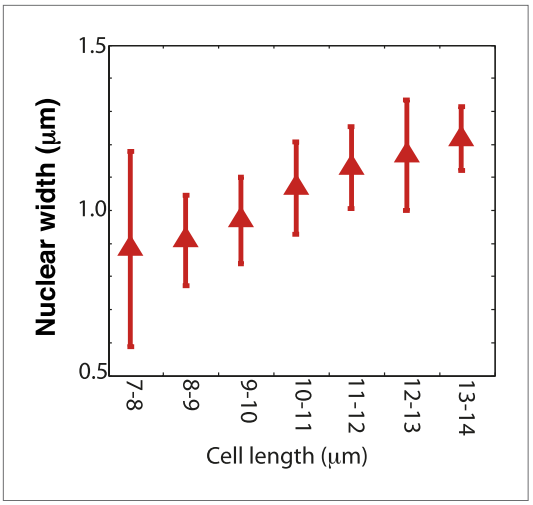

Figure 1—figure supplement 3. Nuclear width as a function of cell length. Nuclear size was measured by the dark nuclear zone of pom1-tomato fluorescence. The width of the nucleus was determined as the maximum distance along the long axis of the cell. n = 96 cells. Error bars = SD. Strain used: FC2054. Note that this method may provide a slight underestimate compared to measurements for instance of a nuclear envelope marker or a diffuse nuclear marker.
DOI: 10.7554/eLife.02040.006

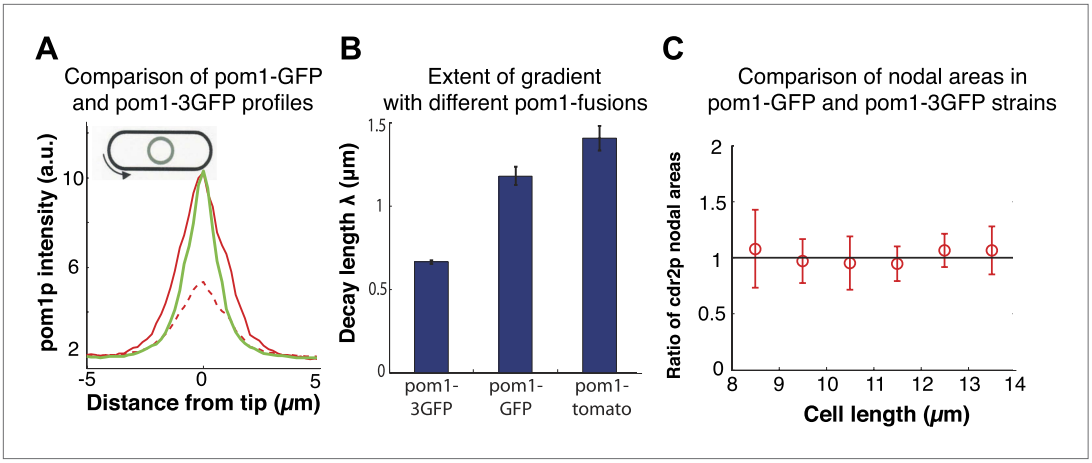

Figure 1—figure supplement 4. Pom1p gradients with different decay lengths do not affect cdr2p distribution. (**A**) Comparison of pom1-3GFP (green, n = 45) and pom1-GFP (red, n = 31) gradients. Dashed red line corresponds to the unscaled pom1-GFP absolute fluorescence values in the cell. The pom1-GFP intensity is adjusted to account for the relative intensity difference (whole cell pom1-3GFP was 2.5 times more intense than pom1-GFP under the same imaging conditions). These data show that these gradients have similar numbers of pom1p molecules at their peaks. Strains used: FC2685, FC1162. Error bars not shown for clarity. (**B**) Fitted decay length of average pom1p intensity profile for three different fluorescent proteins (pom1-3GFP (n = 45 cells), pom1-GFP (n = 31 cells) and pom1-tomato (n = 32 cells)). Strains used: FC2685, FC1162 and FC2054. Note that these cells express the fusion as the only pom1p protein in the cell. Errors are estimated from the fitting of an exponential curve to the average profile for each pom1 fusion. Intensity profiles are normalized to have the same intensity at the cell centers. We have confirmed that different normalizations (and also fitting to the raw data) do not significantly alter the measured decay lengths (data not shown). (**C**) Ratio of distributions of cdr2p nodes in cells with different pom1p gradient distributions. Maximum projection confocal images of cdr2-tomato in pom1-GFP (n = 49 cells) and pom1-3GFP (n = 50 cells) strains were acquired and nodes were specified by a thresholding approach ('Materials and methods'). The ratio is defined as the area of the cdr2p nodes in the pom1-GFP strain divided by the area of the cdr2p nodes in the pom1-3GFP strain. Black line is guide to the eye for ratio of one. Strain used: FC2686. Error bars = SD.
DOI: 10.7554/eLife.02040.007

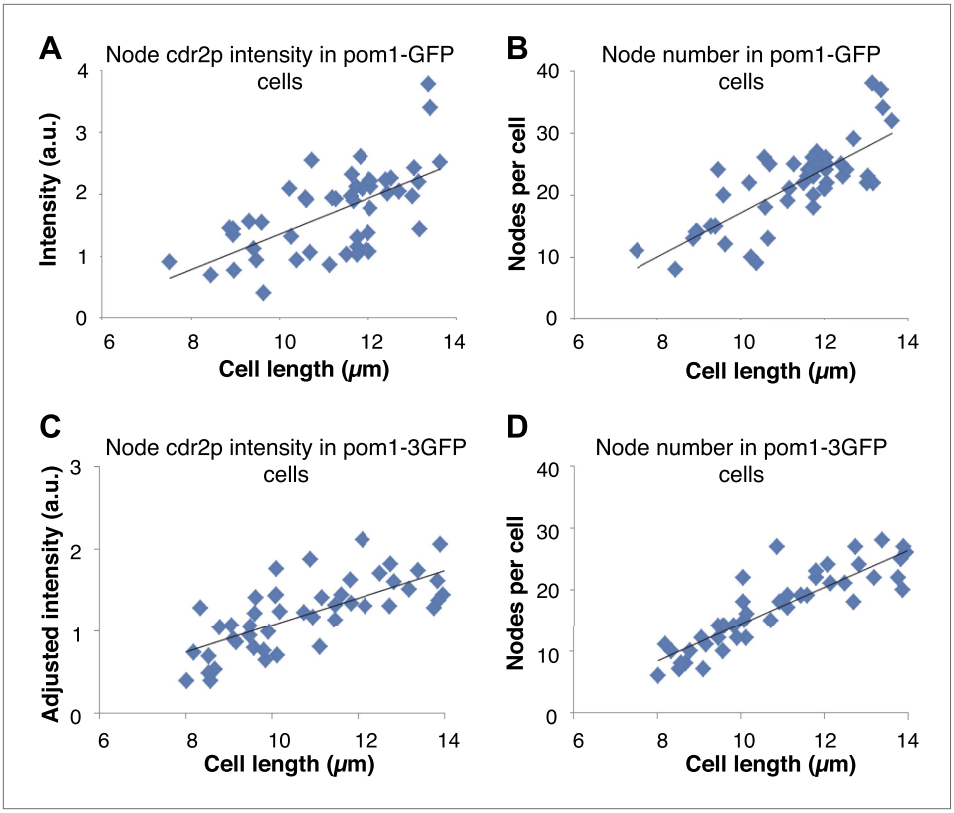

Figure 1—figure supplement 5. Pom1p gradients with different decay lengths do not affect cdr2p node intensity or number. Maximum projection confocal images of cdr2-tomato in pom1-GFP (n = 49 cells) and pom1-3GFP (n = 50 cells) strains were acquired. Nodes were specified by a thresholding approach ('Materials and methods'). Strains used: FC2686, FC2687. (**A**) Intensity of cdr2-tomato in nodes in pom1-GFP strain. Black line is linear best fit (r^2 = 0.39). (**B**) Number of cdr2-tomato nodes in pom1-GFP strain. Black line is linear best fit (r^2 = 0.61). (**C**) Intensity of cdr2-tomato in nodes in pom1-3GFP strain. Note that the intensities were adjusted to be on similar scale to (**A**). Black line is linear best fit (r^2 = 0.55). (**D**) Number of cdr2-tomato nodes in pom1-3GFP strain. Black line is linear best fit (r^2 = 0.80).

DOI: 10.7554/eLife.02040.008

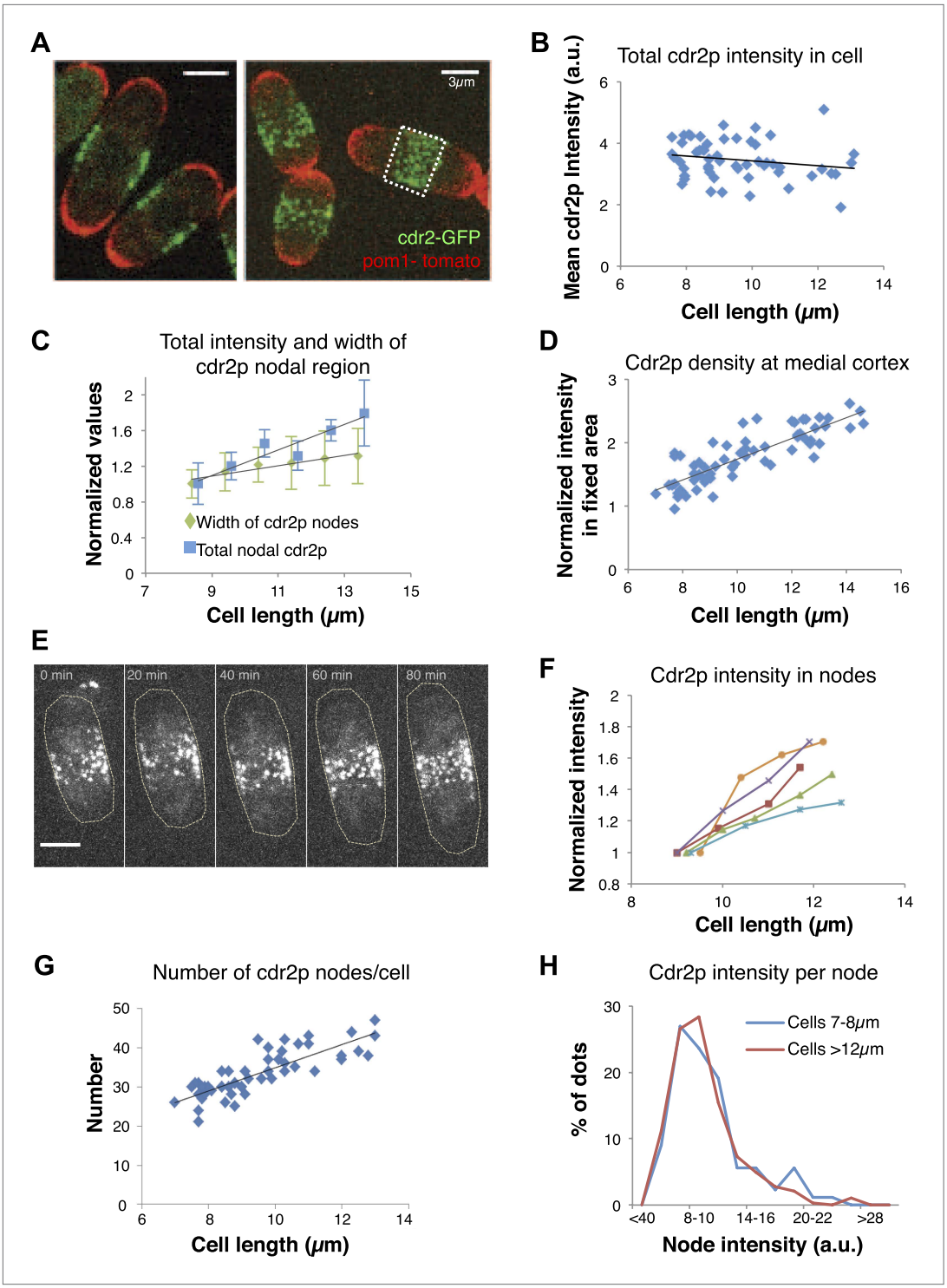

Figure 2. Cdr2p accumulates in nodes at the medial cortex as cells grow. (**A**) Fission yeast cells expressing pom1-tomato and cdr2-GFP. Left panel: single medial confocal section; right panel: maximum Z-projection through whole cell. Strain used: FC2678. Scale bars = 3 μm. (**B**) Total cellular intensity of cdr2-GFP in cells of different lengths. Mean intensities over the whole cell from sum projection images. n = 54 cells. Black line: linear fit with r^2 = 0.04. (**C**) Cdr2-GFP total intensity in medial cortex (blue) (***Figure 2—figure supplement 3A***; n = 51) and width of cdr2-GFP nodal region along long cell axis (green) as function of cell length (n = 185). Error bars = SEM. Black lines: linear fits, r^2 = 0.90 and 0.89 for width and intensity respectively. See ***Figure 2—figure supplements 1–4***. (**D**) Total cdr2-GFP intensity in fixed a 3-μm wide medial band as function of cell length (***Figure 2—figure supplement 3F***) n

Figure 2. Continued on next page

Figure 2. Continued

= 67. Black line: linear fit with r^2 = 0.71. (**E**) Time-lapse maximum projection images of a cell expressing cdr2-GFP. Scale bar = 3 μm. (**F**) Total normalized intensities of nodal cdr2-GFP in 5 cells tracked over time (measured from images like **E**, using method of ***Figure 2—figure supplement 3A***). See ***Figure 2—figure supplement 5***. (**G**) Number of cdr2-GFP nodes as function of cell length (n = 51). Black line: linear fit with r^2 = 0.67. Nodes identified by thresholding, using method of ***Figure 2—figure supplement 3C***, which provides a lower-bound estimate. (**H**) Distributions of cdr2-GFP node intensities in short vs long cells. n = 89 nodes in 9 cells, n = 286 nodes in 7 cells, respectively (nodes as determined in **G**).

DOI: 10.7554/eLife.02040.009

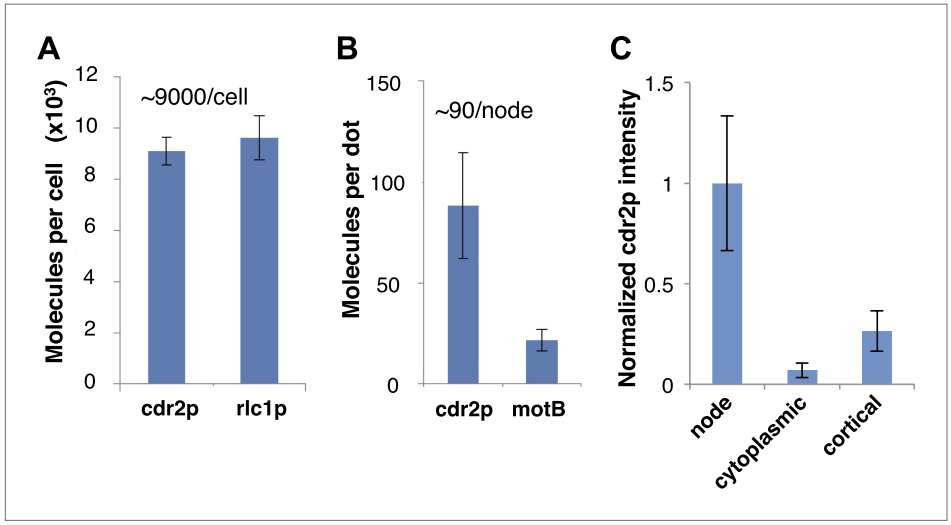

Figure 2—figure supplement 1. Measurement of cdr2p protein number. (**A**) Protein numbers were estimated by comparison of fluorescence intensity in living cells with standard fusion proteins that have been quantitated previously. Quantification of average cdr2p molecules in the whole cell was estimated by comparing total cell fluorescent intensity of cdr2-GFP with rlc1-GFP (regulatory light chain of myosin), which has been estimated around 9600 molecules/cell (Wu and Pollard, 2005) (n = 50 cells). Strains used: FC2688, FC1139. Error bars = SD. (**B**) Quantification of cdr2p molecules in each node by comparing cdr2-GFP with the *E. coli* flagellar protein motB-GFP expressed in bacteria, estimated to be 22 molecules/dot (***Coffman et al., 2011***) (n = 200 nodes). Error bars = SD. (**C**) Comparison of fluorescence intensities of different cdr2-GFP species, using images of cdr2-GFP cells in a single medial slice. The cdr2-GFP mean intensities in a 12 pixel square area in a cdr2p node, cytoplasm, and dim cortical dots outside of the medial cortex were measured (***Figure 5A***). Note that only the brighter, more discrete cortical dots were assayed. n = 20 measurements each in >5 cells. Error bars = SD.

DOI: 10.7554/eLife.02040.010

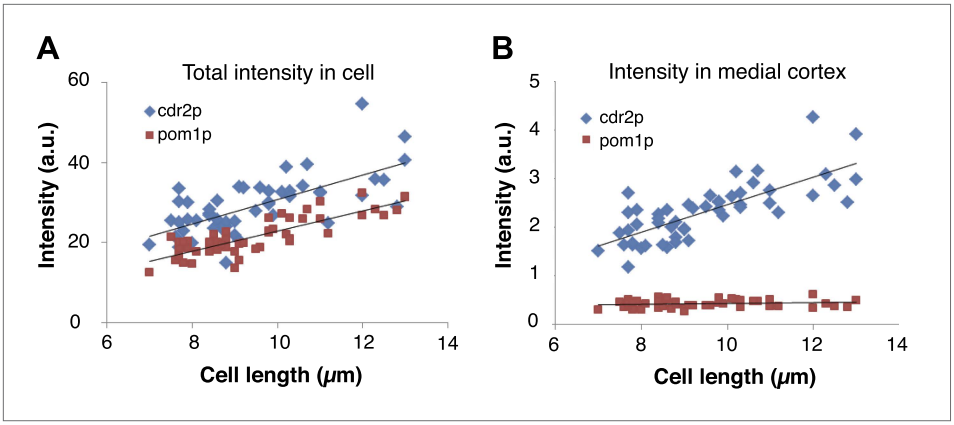

Figure 2—figure supplement 2. Cdr2p and pom1p intensity measurements as a function of cell length. (**A**) Total intensity of cdr2-GFP and pom1-tomato in the cell as a function of cell length using maximal projection images. Black lines are linear best fits. Intensities were measured by a hand drawn region of interest (ROI) around the entire cell in a maximal projection of a stack of 13 confocal sections 0.4 μm apart. Strain used: FC2678. n = 50 cells. (**B**) Intensity of cdr2-GFP and pom1-tomato in the medial cortex as a function of cell length. Intensities were measured from the same maximal projection as (**A**) but with a hand drawn ROI around the cortical band area. n = 50 cells.
DOI: 10.7554/eLife.02040.011

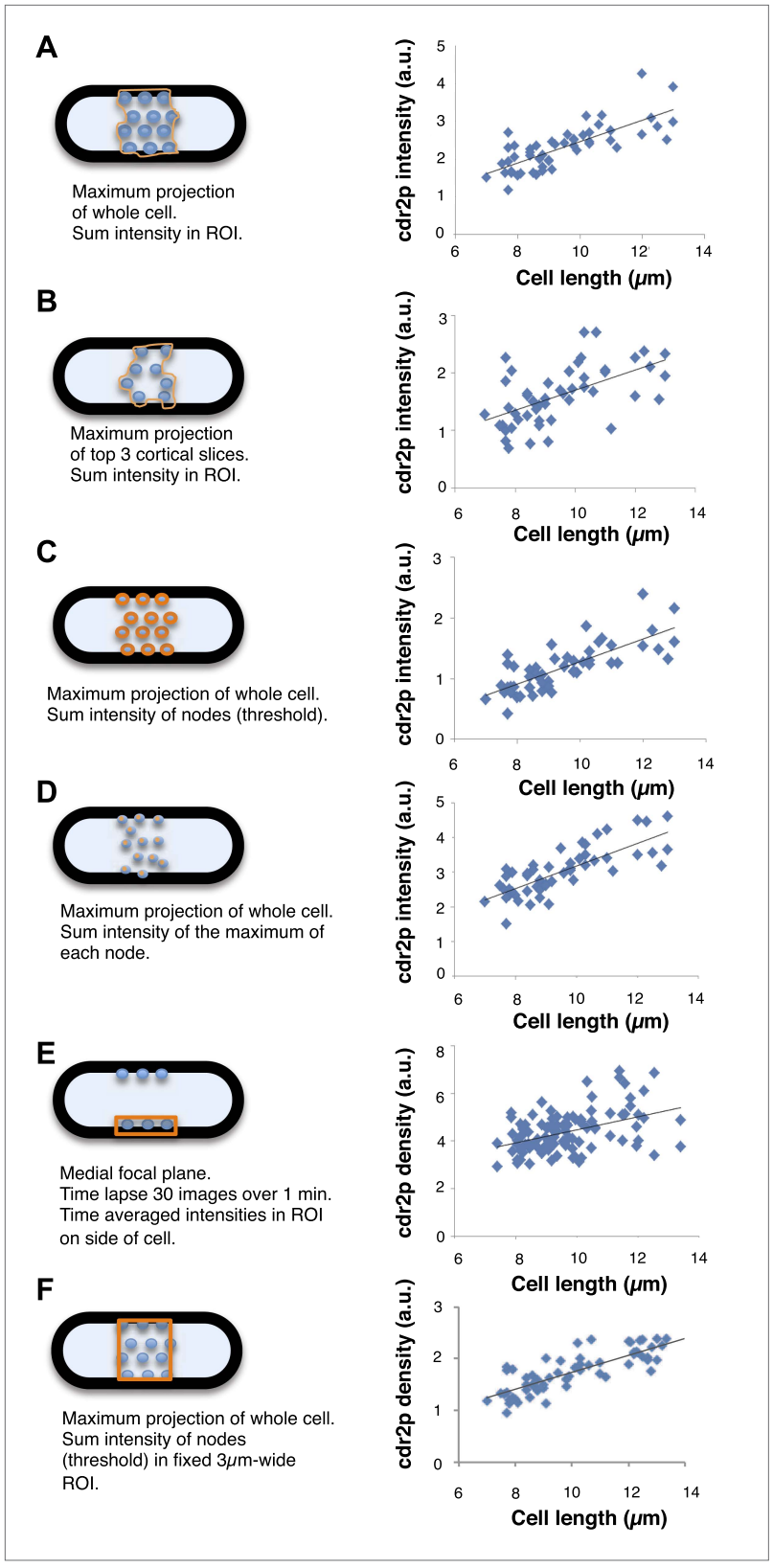

Figure 2—figure supplement 3. Comparison of image analysis methods for quantitating cdr2p fluorescence in the nodes. Different methods to image and

Figure 2—figure supplement 3. Continued on next page

Figure 2—figure supplement 3. Continued

analyze cdr2p intensities were compared. The details of each method are presented in the figure and described in detail in the 'Materials and methods'. Graphs show results of each method on cdr2p medial node intensity vs cell length in a population of cells. The intensities are normalized relative for each data set. All show a similar scaling of cdr2p node intensity with cell length. n = 49 cells.

DOI: 10.7554/eLife.02040.012

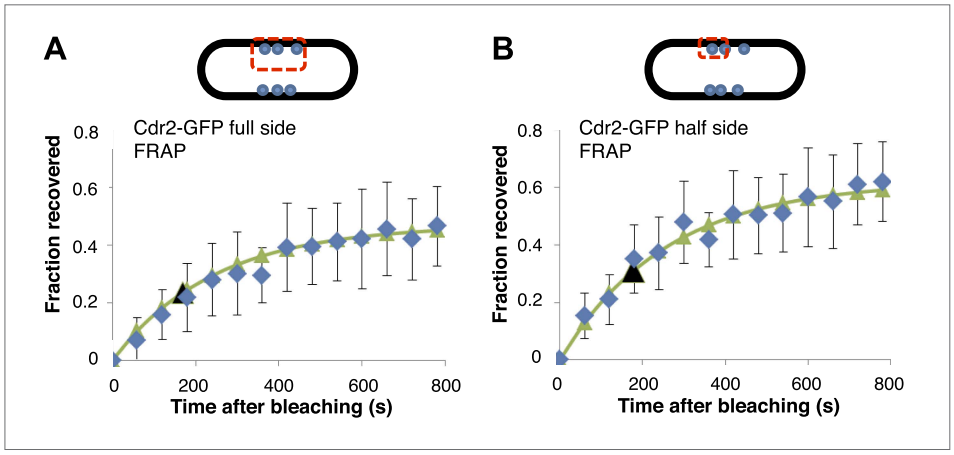

Figure 2—figure supplement 4. FRAP analysis of cdr2-GFP. Cdr2-GFP in the nodes was photo-bleached in the indicated regions, and fluorescence recovery was monitored over time. Cells were imaged in a single medial focal plane. Average data (blue) were fitted to exponential curves (green). The black arrows indicate the time of 50% recovery. $t_{1/2}$ was about 3 min for both sets of data. The similar rates of recovery for the full side and half side bleach patterns suggest that there is little exchange of cdr2-GFP between nodes. n = 14 cells (**A**), n = 8 cells (**B**). Strain used: FC1441. Error bars = SD in both panels.

DOI: 10.7554/eLife.02040.013

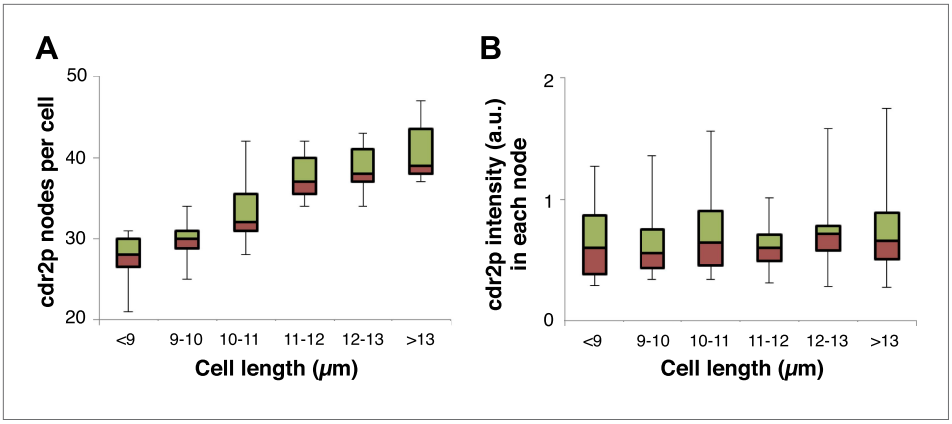

Figure 2—figure supplement 5. Cdr2p node number but not maximal intensity in each node increases with cell length. Cdr2-GFP in each node was measured by the ImageJ 'Find Maxima' function, and data was graphed in bins according to cell length. (**A**) shows a rise in the number of cdr2-GFP nodes with cell length. (**B**) shows the intensity of cdr2-GFP in each node does not increase on average. Note that this thresholding method underestimates the number of nodes slightly. cdr2-GFP intensity measured as defined in (***Figure 2—figure supplement 3A***). Strain used: FC1441. n = 51.

DOI: 10.7554/eLife.02040.014

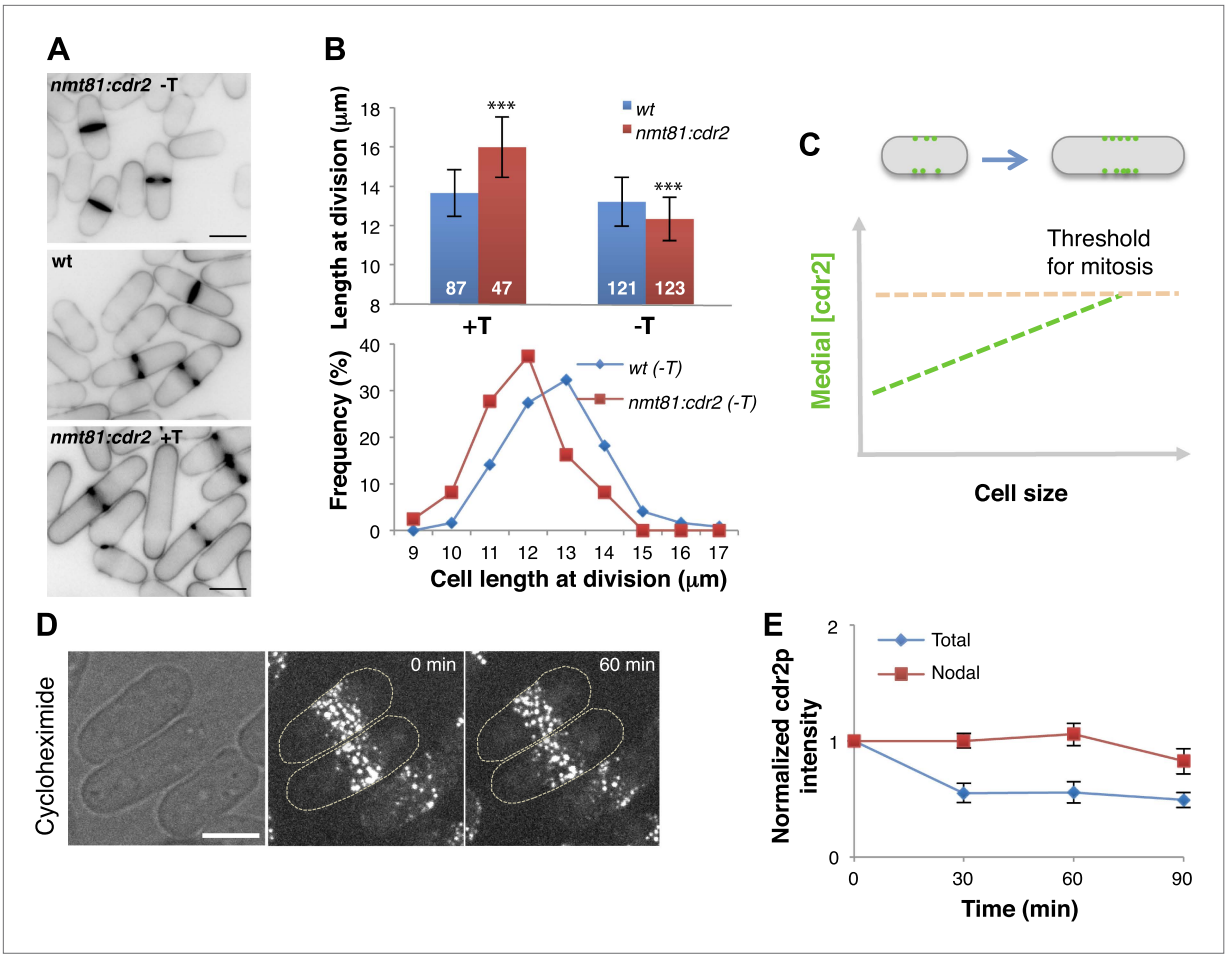

Figure 3. Cdr2p is a dose-dependent regulator of cell size. (**A**) Effect of cdr2p expression level on cell size. *cdr2*$^{+}$ was expressed at different levels using a thiamine-regulatable promoter (*nmt81-cdr2*). Inverted images of cells stained with cell wall dye blankofluor. Cells express cdr2p at levels on average of 1.6, 1.0 and 0.3-fold relative to wild type (top to bottom). Strains used: FC15, FC2691. Scale bar = 5 μm. (**B**) Length of cells at septation. n = 87, 47, 121, 123 cells. T = thiamine. Error bars = SD, ***p<0.0001 as determined by Kolmogorov–Smirnov statistical tests. (**C**) Model that the local concentration of cdr2p increases in the region of the medial cortical nodes as cells grow, and when it reaches a critical level, promotes entry into mitosis. (**D**) Stability of cdr2-GFP protein. Time-lapse images of cells expressing cdr2-GFP treated with 100 μg/ml cycloheximide (***Polanshek, 1977***). Strain used: FC2688. Scale bar = 5 μm. (**E**) Total cell and nodal cdr2-GFP intensities in individual cells treated with cycloheximide over time. Total cell intensity was measured as in ***Figure 2B*** n = 9 cells. Error bars = SD.

DOI: 10.7554/eLife.02040.016

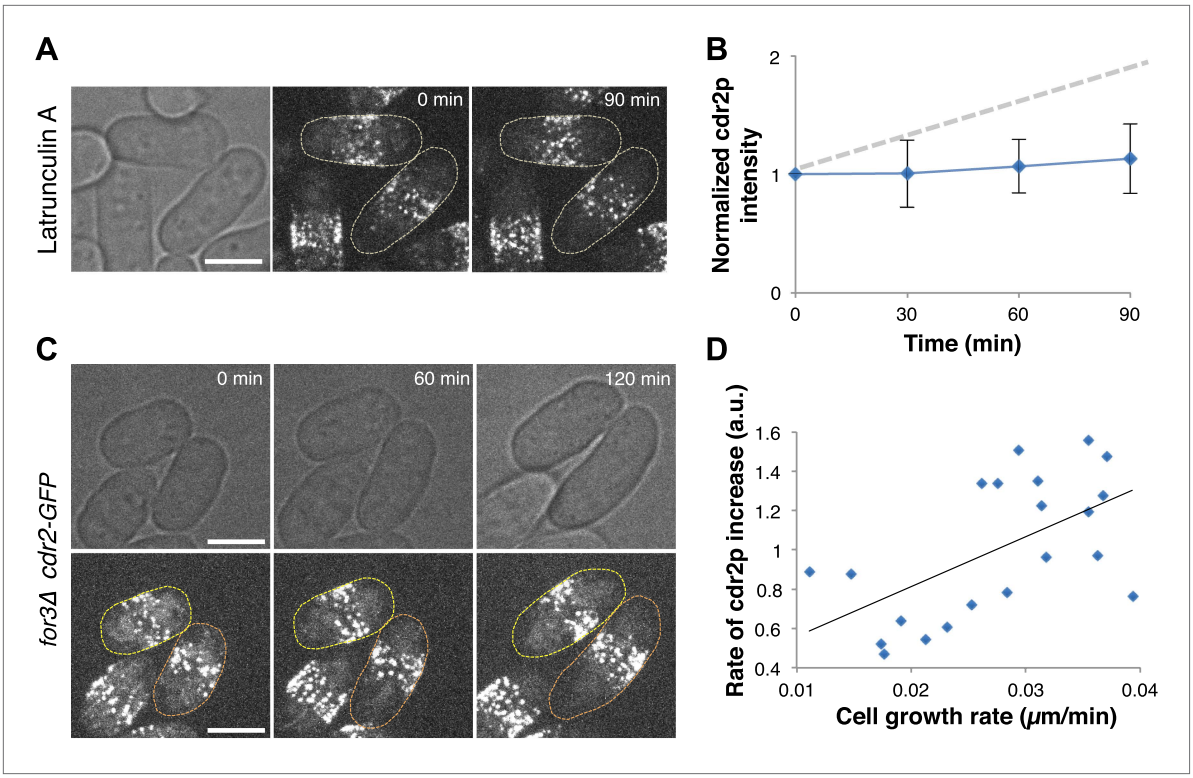

Figure 4. Cdr2p has properties of a sizer but not a timer. (**A**) Cdr2-GFP does not accumulate at nodes over time without cell growth. Time lapse images of cells in which growth was halted by 200 μM Latrunculin A, an actin inhibitor (***Chang, 1999***). Scale bar = 5 μm. Strain used: FC2688. (**B**) Mean cdr2-GFP nodal intensity over time in individual LatA-treated cells. n = 9 cells. Error bars = SD. Dotted line shows for comparison the observed average increase of nodal cdr2-GFP in untreated, growing cells (from ***Figure 2F***). (**C**) Time-lapse images of cdr2-GFP in *for3Δ* (formin) cells. Two sister cells which exhibit variable growth rates are highlighted (yellow and orange outlines). Strain used: FC2690. Scale bar = 5 μm. (**D**) Correlation between cell growth rate and the rate of accumulation of cdr2-GFP in *for3Δ* cells (***Figure 4—figure supplement 1***). Line is linear fit to the data (r^2 = 0.34). A 'timer' molecule would show no correlation. n = 21 cells.

DOI: 10.7554/eLife.02040.017

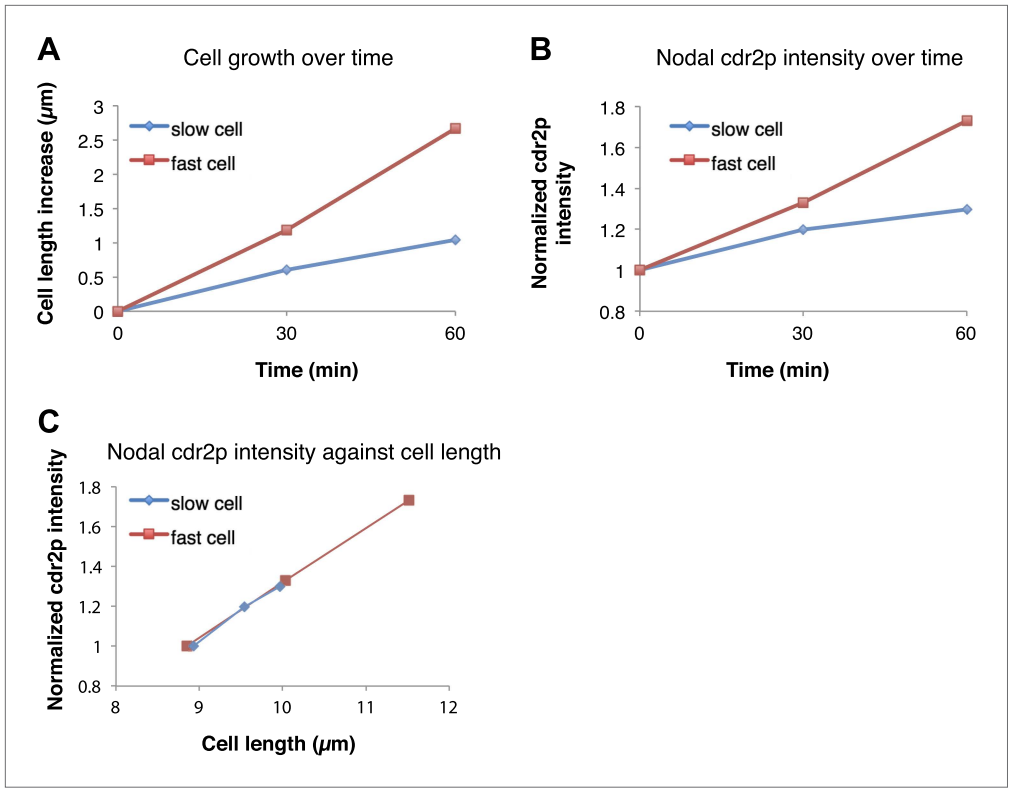

Figure 4—figure supplement 1. Rate of cdr2p nodal accumulation correlates with the rate of cell growth. The effect of cell growth rate on cdr2p accumulation was examined by analyzing for3 (formin) mutant cells, which exhibit highly variable growth rates (***Feierbach and Chang, 2001***). Strain used: FC2690. (**A**) Cell growth over time in a representative slow and fast-growing cell. (**B**) Cdr2-GFP nodal accumulation over time as measured by fluorescence intensity in the same two cells. Cdr2-GFP measurement method described in 'Materials and methods'. (**C**) Plot of cdr2-GFP increase as a function of cell length increase in the same two cells. These data suggest that cdr2p increases scale with cell size increases rather than time. See ***Figure 4*** for results of the full data set.
DOI: 10.7554/eLife.02040.018

A

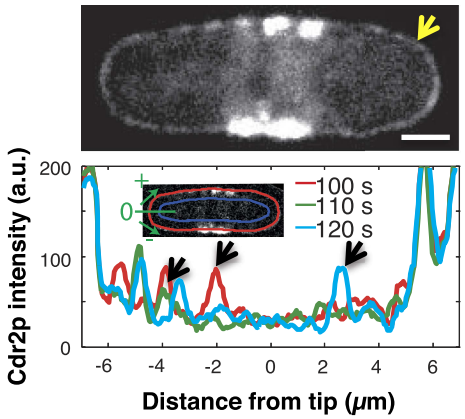

B

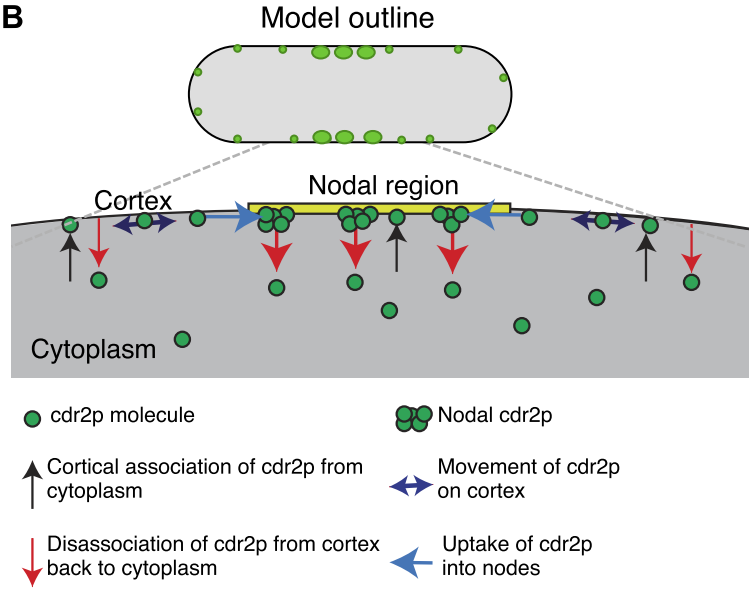

C

Model equations at quasi-steady state:

$$0 = \beta \frac{A_{cor}}{V} N_{cyt} - \nu N_{cor} - \alpha \frac{A_{nod}}{A_{cor}} N_{cor}$$

$$0 = \alpha \frac{A_{nod}}{A_{cor}} N_{cor} - \eta N_{nod}$$

where N_{cyt}, N_{cor} and N_{nod} are cdr2p molecule number in the cytoplasm, cortex and nodal regions respectively and V is the cytoplasm volume.

Solutions:

$$\rho_{nod} = \rho_{cyt} \frac{\beta}{\eta} \left(\frac{\nu}{\alpha} + \frac{A_{nod}}{A_{cor}} \right)^{-1} \propto \frac{A_{cor}}{A_{nod}} \quad \text{if } \frac{\nu}{\alpha} \ll 1$$

$$\rho_{cor} = \frac{\eta}{\alpha} \rho_{nod} \ll \rho_{nod} \quad \text{if } \frac{\eta}{\alpha} \ll 1$$

where $\rho_{cyt} = N_{cyt}/V$ is the cytoplasmic cdr2p concentration and $\rho_{nod} = N_{nod}/A_{nod}$ $\rho_{cor} = N_{cor}/A_{cor}$

D

Parameter	Symbol	Value	
Cortical area	A_{cor}	~70–150μm^2	Measured
Nodal area	A_{nod}	~20–25μm^2	Measured
cdr2p cortical association	β	0.02μms^{-1}	Not important
cdr2p cortical disassociation	ν	0.005s^{-1}	Constrained
cdr2p nodal uptake	α	1.0s^{-1}	Constrained
cdr2p nodal disassociation	η	0.005s^{-1}	Measured

E

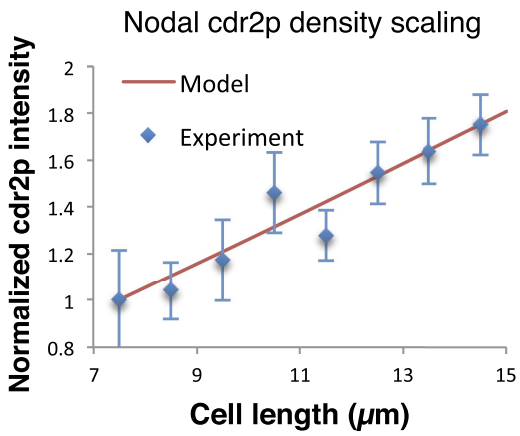

Figure 5. Model for cell size-sensing by cdr2p. (**A**) Confocal time-averaged image (60 frames over 10 min) in medial focal plane of cell expressing cdr2-GFP. Arrow highlights dim cdr2-GFP all around cell cortex (***Video 2***). Scale bar = 2 μm. Graph shows cdr2-GFP profiles on cortex around one pole

Figure 5. Continued on next page

Figure 5. Continued

at indicated time points. Cdr2-GFP appears brighter in the cytoplasm around nodes due to out-of-focus nodal fluorescence. Black arrows denote local peaks in the cdr2-GFP signal that are clearly distinct from the mean cdr2-GFP cortical signal. Strain: FC2678. (**B**) Outline of mathematical model for cdr2p dynamics. (**C**) Equations and analytic solutions describing cortical and nodal cdr2p number. (**D**) Model parameters. 'Measured': deduced directly from experiment, 'constrained': limited by nodal cdr2p density scaling with cell length, 'not important': plays no role in nodal cdr2p density scaling. (**E**) Model fit to nodal cdr2-GFP density as function of cell length (data from maximum intensity projection as described in ***Figure 2—figure supplement 3A***, with cells binned by length at 1 μm intervals). Equations and parameters given in **C**, **D**. Error bars = SD. See ***Figure 5—figure supplement 1, 2***.

DOI: 10.7554/eLife.02040.019

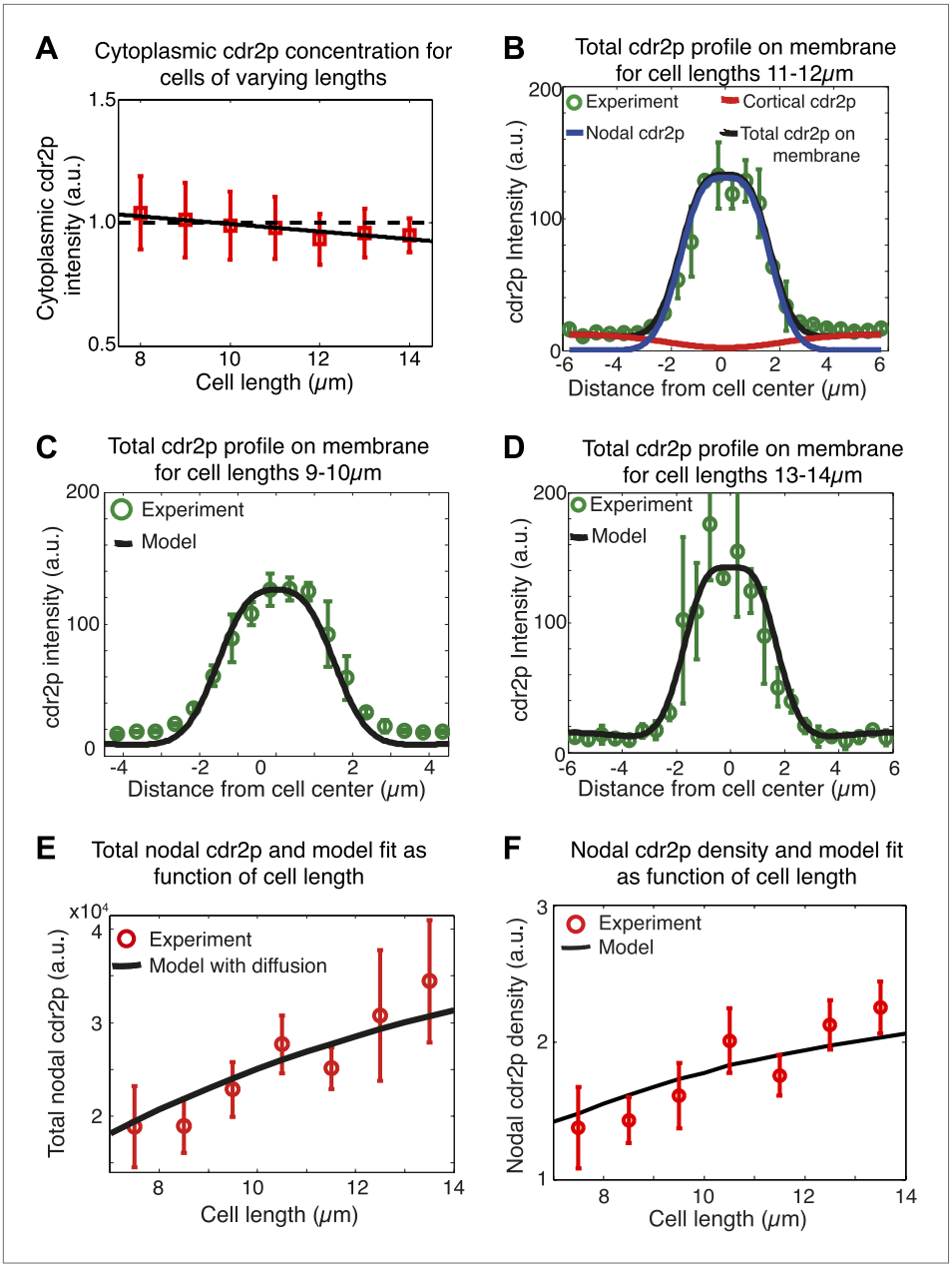

Figure 5—figure supplement 1. Spatial membrane model for cdr2p distribution. (**A**) Measured cytoplasmic cdr2-GFP intensity (n = 267) as function of cell length. Solid black line is best linear fit and dashed line is best fit to data assuming constant cytoplasmic cdr2p levels. Error bars are SD. (**B**) Model fit (black line) to experimentally measured cdr2-GFP intensity profile on the membrane (for cells of length 11–12 μm) (green circles), where the model contributions from the nodal (blue) and cortical (red) cdr2p are also shown. Average profile obtained from individual time-averaged cdr2-GFP profiles over 90 s around nodal region in confocal section through the middle of each cell. (**C**) as (**B**), but for shorter cells (9–10 μm). (**D**) as (**B**) but for longer cells (13–14 μm). n > 20 in **B**, **C** and **D**. (**E**) Model fit for the increase in total nodal cdr2p with cell growth, including cortical cdr2p diffusion, compared to experimental data. Data shown is for a subset of the experimental results shown in ***Figure 5E*** (n = 39). (**F**) Similar to ***Figure 5E***, except model fit is for the increase in nodal cdr2p density (defined as mean concentration in 3-μm region about cell center) with cell growth, including cortical cdr2p diffusion. Data shown is for a binned subset of data shown in ***Figure 2—figure supplement 3F*** (n = 39).

DOI: 10.7554/eLife.02040.020

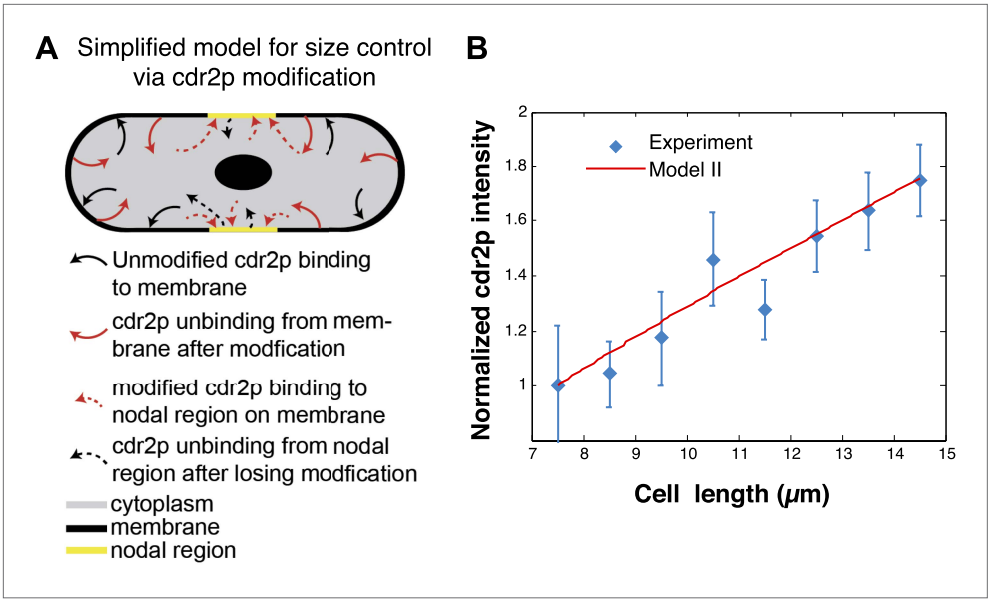

Figure 5—figure supplement 2. Cdr2p-modification model. (**A**) Simplified schematic of a model for cdr2p scaling involving cdr2p-modification. Unmodified cdr2p rapidly diffuses in the cytoplasm. Cdr2p can bind (black arrows) to the membrane. On the membrane, cdr2p can be modified and subsequently unbinds from the membrane (red arrows). This modified form of cdr2p can rapidly diffuse through the cytoplasm and bind (dashed red arrows) to the nodal regions on the membrane (yellow region). Unbinding of modified cdr2p from the nodal region back to an unmodified form of cdr2p in the cytoplasm is denoted by dashed black arrows. For clarity we do not depict spontaneous reversion of modified cdr2p back to unmodified cdr2p in the cytoplasm. (**B**) Scaling of nodal cdr2p concentration in the cdr2p-modification model (for parameters given in 'Materials and methods'), where nodal cdr2p concentration is normalized to 1 at cell length 7.5 μm. Experimental data are same as ***Figure 5E***. Strain used: FC2678.

DOI: 10.7554/eLife.02040.021

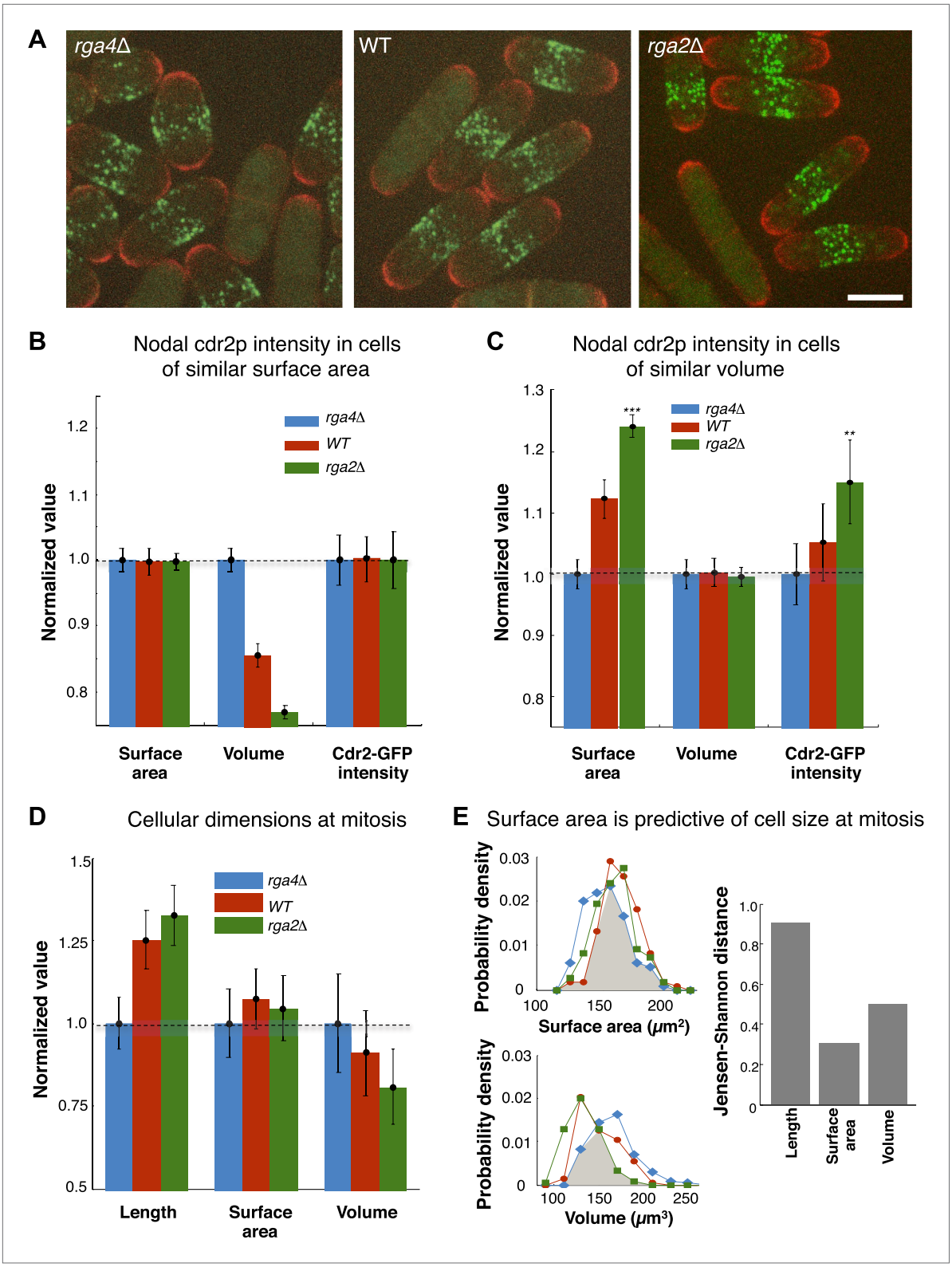

Figure 6. Cdr2p and cell size at division scale with cell surface area. (**A**) Fission yeast cells expressing cdr2-GFP and pom1-tomato in wt, *rga4*Δ (fat morphology) and *rga2*Δ (thin morphology) backgrounds. Maximum Z-projection images. Cells lacking nodes are in mitosis. Strains used: FC2678, FC2794, FC2795. Scale bar = 5 μm. (**B**) Comparison of measured nodal Cdr2-GFP intensity in cells of different volumes. For each cell, the surface area and volume were measured by segmentation ('Materials and methods'). A subset of cells whose surface area was within 10–20% of the mean surface

Figure 6. Continued on next page

Figure 6. Continued

area was selected for each cell type ('Materials and methods'). The graphs show the surface area, volume, and nodal cdr2-GFP intensity (cdr2-GFP intensity measured as defined in ***Figure 2—figure supplement 3A***) in these selected cells. For each data type, normalization is by mean value for *rga4*Δ cells. Error bars = Error on the mean. n = 24 (wt) cells, 27 (*rga4*Δ), 32 (*rga2*Δ). Strains used in **B** and **C**: FC1441, FC2792, FC2793. See ***Figure 6—figure supplement 1***. (**C**) As in **B**, except groups of cells were selected with similar volumes (mean measured volume ± 10–20%). n = 24 (wt) cells, 27 (*rga4*Δ), 27 (*rga2*Δ). These data show cdr2-GFP scaling with surface area. The difference in surface area and cdr2-GFP intensity between the *rga2*Δ and *rga4*Δ cells is statistically significant (**$p<10^{-3}$, ***$p<10^{-4}$). See ***Figure 6—figure supplement 1***. (**D**) Comparison of cell lengths, surface areas and volumes in *rga4*Δ, wild type and *rga2*Δ at time of septation ('Materials and methods'). The septum is not included in these measurements. Data for each set is normalized by the appropriate value for the *rga4*Δ cells. Error bars = SD. Strains used: FC2554, FC2555, FC2556. n = 76 (wt), 64 (*rga4*Δ), 60 (*rga2*Δ). (**E**) Quantitating differences between *rga4*Δ, wt and *rga2*Δ at time of septation. Left: probability density distributions for measured surface area (top) and volume (bottom) for wild type (red), *rga2*Δ (green) and *rga4*Δ (blue) cells in (**D**). Gray area marks the overlap region between the distributions. Error bars not shown for clarity. Right: to quantitatively compare these distributions, we calculated the Jensen–Shannon distance (***Lin, 1991***) between the length, surface area and volume distributions for the different cell types (where 1 corresponds to the distributions having no shared information and 0 to identical distributions, see 'Materials and methods'). This analysis shows that these cells with different shapes divide with similar surface area.

DOI: 10.7554/eLife.02040.023

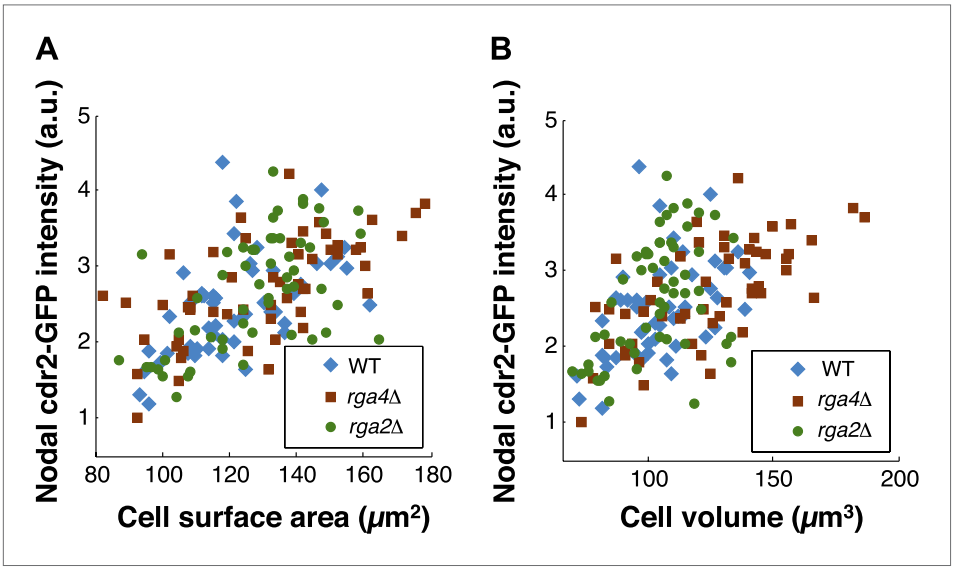

Figure 6—figure supplement 1. Scaling of nodal cdr2-GFP intensity with surface area and volume. (**A**) Nodal cdr2-GFP intensity from maximum intensity projection for wt, rga4Δ (fat cells), and rga2Δ (thin cells) plotted against cell surface area. (**B**) Nodal cdr2-GFP intensity from maximum intensity projection for wt, rga4Δ (fat cells), and rga2Δ (thin cells) plotted against cell volume. Strains used: FC1441, FC2792, FC2793. n = 51 (wt), 54 (rga4Δ), 58 (rga2Δ).

DOI: 10.7554/eLife.02040.024

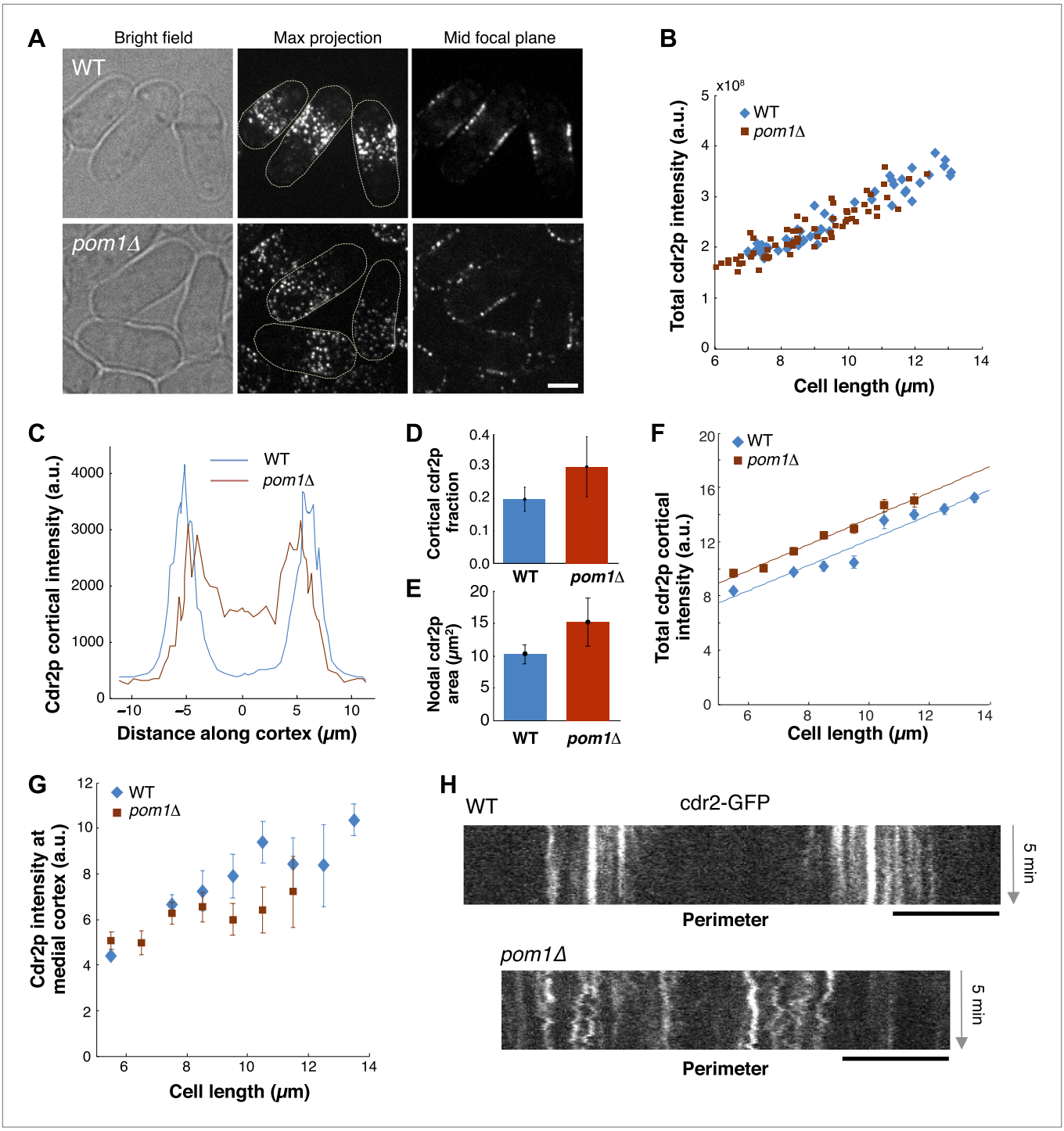

Figure 7. Cdr2p behavior in *pom1Δ* mutants. (**A**) Fission yeast cells expressing Cdr2-GFP in wt and *pom1*Δ background. Brightfield, maximum projection, and mid–focal plane images are shown. Strains used: FC1441 and FC2057. Scale bar = 3 μm. (**B**) Comparison of total measured cdr2-GFP intensity (from sum projection after background subtraction) with cell length. n = 52 (wt), 72 (*pom1*Δ). (**C**) Average cdr2-GFP intensity profile around cortex of cell (spatial direction as defined in cartoon in ***Figure 1F***). *pom1Δ* cells are orientated such that the cell end with the higher cdr2-GFP level is defined to be at d = 0 μm. n = 52 (wt) cells, 72 (*pom1*Δ). Error bars not shown for clarity. See 'Materials and methods' for further details. (**D**) Fraction of cdr2-GFP signal observed on the cortex compared with total measured cdr2-GFP in the medial plane. The cortical signal is calculated as the sum of measured intensity along a mask around the cortex (see 'Materials and methods' for mask definition). The total signal is defined as the total measured cdr2-GFP intensity on and inside the mask. Error bars = SD. n = 52 cells (wt), 72 (*pom1*Δ). (**E**) Measured area of nodal cdr2-GFP region from maximum intensity projection images. Regions were measured manually for individual cells. n = 46 (wt) cells, 77 (*pom1*Δ). Error bars = SD. (**F**) Accumulation of total membrane

Figure 7. Continued on next page

Figure 7. Continued

cdr2-GFP (both nodal and cortical signal) against cell length. n = 52 (wt) cells, 72 (*pom1*Δ). See 'Materials and methods' for details. Lines are linear least-square fits to the data, with similar slopes. Error bars = SD. (**G**) Accumulation of nodal cdr2-GFP (maximum intensity projection) within 3 μm medial cortical region. n = 52 cells (wt), 72 (*pom1*Δ). Error bars = SD. (**H**) Kymograph of cortical cdr2-GFP over 5-min period in wild type and *pom1*Δ cells. Scale bars = 5 μm.

DOI: 10.7554/eLife.02040.025

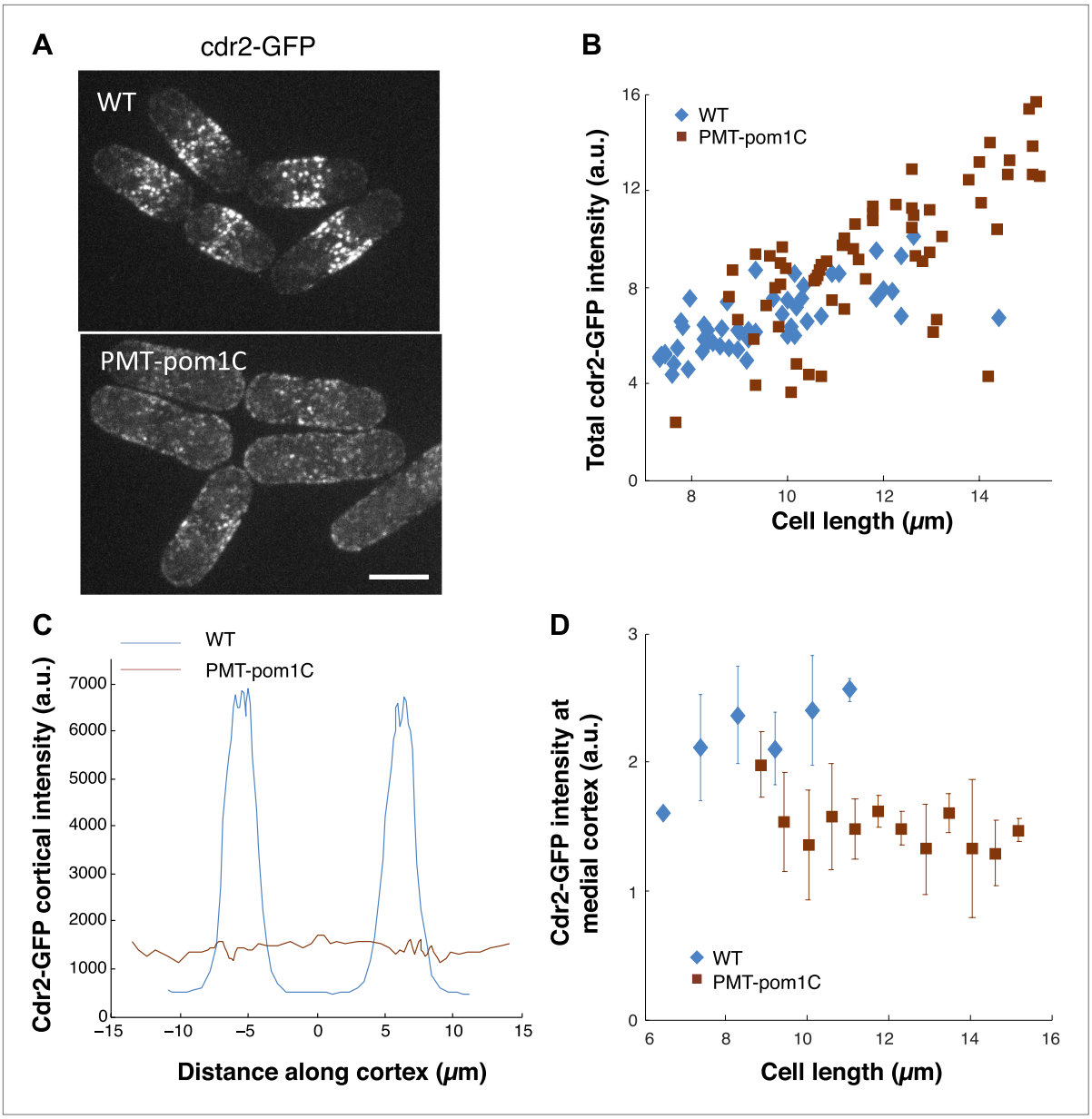

Figure 7—figure supplement 1. Cdr2p behavior in cells in which pom1p is targeted all over the cortex. (**A**) Fission yeast cells expressing cdr2-GFP in wild-type and PMT-pom1C cells in which a pom1p chimera is localized throughout the cortex. Maximum Z-projection images are shown. Strains used: JM2057, JM892. Scale bar = 5 μm. (**B**) Total cdr2-GFP intensity in cells (n = 64 [wt], 54 [PMT-pom1C]). Method is same as in ***Figure 7B***. (**C**) Average cortical profile of cdr2-GFP intensities from maximum intensity projection (distance defined as in cartoon in ***Figure 1F***). See 'Materials and methods' for mask definition. Error bars are not shown for clarity. n = 64 (wt), 54 (PMT-pom1C). (**D**) Intensity of cdr2-GFP in a 3-μm wide region of the medial cortex as function of cell length. Data from maximum intensity projection images. n = 64 (wt), 54 (PMT-pom1C). Error bars = SD.

DOI: 10.7554/eLife.02040.026